Reduced graphene oxide modified smart conducting paper for Cancer biosensor

Saurabh Kumar, Suveen Kumar, Saurabh Srivastava, Birendra K. Yadav, Seung H. Lee, Jai G. Sharma, Dinesh C. Doval, Bansi D. Malhotra

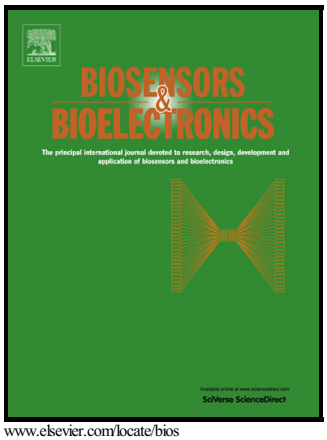

www.elsevier.com/locate/bios

PII: S0956-5663(15)30136-6
DOI: http://dx.doi.org/10.1016/j.bios.2015.05.040
Reference: BIOS7702

To appear in: *Biosensors and Bioelectronic*

Received date: 3 March 2015
Revised date: 16 May 2015
Accepted date: 17 May 2015

Cite this article as: Saurabh Kumar, Suveen Kumar, Saurabh Srivastava, Birendra K. Yadav, Seung H. Lee, Jai G. Sharma, Dinesh C. Doval and Bansi D. Malhotra, Reduced graphene oxide modified smart conducting paper for Cancer biosensor, *Biosensors and Bioelectronic,* http://dx.doi.org/10.1016/j.bios.2015.05.040

Reduced Graphene Oxide Modified Smart Conducting Paper for Cancer Biosensor

Saurabh Kumar,[a] Suveen Kumar,[a] Saurabh Srivastava,[a] Birendra K. Yadav,[b] Seung H. Lee,[c] Jai G. Sharma,[a] Dinesh C. Doval,[b] and Bansi D. Malhotra*,[a]

[a] Nanobioelectronics Laboratory, Department of Biotechnology, Delhi Technological University, Shahbad Daulatpur, Delhi-110042, India

[b] Rajiv Gandhi Cancer Institute and Research Centre, Rohini, Delhi-110085, India

[c] Applied Materials Institute for BIN Convergence, Department of BIN Fusion Technology, Chonbuk National University, Jeonju 561-756, Korea

Corresponding author: Bansi Dhar Malhotra, Email: bansi.malhotra@gmail.com,

Phone: +11 27871043 or 91 11 27871022 Extension:1609;

Abstract

We report results of the studies relating to the fabrication of a paper based sensor comprising of poly (3,4-ethylenedioxythiophene):poly(styrenesulfonate) (PEDOT:PSS) and reduced graphene oxide (RGO) composite. The effect of various solvents like methanol, ethylene glycol and H_2SO_4 on the electrical conductivity of PEDOT: PSS coated Whatman paper has been investigated. The conductivity of this solution processed conducting paper significantly increases from ~1.16×10^{-4} Scm^{-1} up to ~3.57×10^{-2} Scm^{-1} (~300 times) on treatment with ethylene glycol. The observed significant increase in electrical conductivity is due to conformational rearrangement in the polymer and due to strong non-covalent cooperative interaction between PEDOT and the cellulose molecules. Further, incorporation of RGO into the conducting paper results in improved electrochemical performance and signal stability. This paper electrode is a promising alternative over the expensive conventional electrodes (ITO, gold and glassy carbon),

that are known to have limited application in smart point-of-care (POC) devices. This low cost, flexible and environment friendly conducting paper based biosensor utilized for cancer biomarker (carcinoembryonic antigen, CEA) detection, reveals high sensitivity of 25.8 $\mu Ang^{-1}mLcm^{-2}$ in the physiological range, 1-10 $ngmL^{-1}$.

Keywords: Conducting Paper, PEDOT: PSS, Biosensor, Cancer

1. Introduction

Paper based point-of-care (POC) devices are rapidly evolving for desired analytical and clinical applications since these are predicted to be simple, cost-effective, portable, consume low power and are disposable. These devices have potential applications in healthcare, detection of toxicants, explosives and environmental studies. Compared to conventional laboratory assays, these devices are found to be very helpful for making speedy decision for therapeutics. Besides this, the testing can be performed near the vicinity of a patient and hence these devices have recently gained much attention in health care. (Gervais et al. 2011; Kumar et al. 2013a; Kumar et al. 2013b; Luppa et al. 2011)

Electrochemical sensors are known to play an important role in on-going transition towards the paper based POC diagnostic devices. The electrochemical techniques offer high sensitivity, high signal-to-noise ratio, portability and fast response time. (Wang 2006) Therefore, its integration with the paper may be advantageous. To ensure the application of paper in an electrochemical sensor, it is essential to make it conducting. In this context, many methods such as screen printing, inkjet printing etc. have been used to incorporate conducting ink on a paper substrate.(Jagadeesan et al. 2012; Tobjörk and Österbacka 2011) These methods require complex fabrication steps, additional instrumentation, skilled personnel and are time-consuming.

Conducting polymers (CPs) have been considered a promising candidate to obtain conducting paper due to delocalization of π electrons since they are known to facilitate rapid electron transfer, mechanical flexibility and solution processability. Doping of a conducting polymer has been found to enhance its electronic, optical, physical, chemical and electrochemical properties. (Dhand et al. 2011) CPs have been predicted to have enough potential for the development of a low cost and high performance biosensor materials that offer high permeability to a given biomolecule, biocompatibility, and rapid electron transfer. (Li et al. 2015; Zhai et al. 2013) Among the various conducting polymers, poly(3,4ethylenedioxythiophene): poly(styrenesulfonate) (PEDOT:PSS) has been considered to be a interesting candidate for development of a conducting paper due to its homogeneous entrapment in/on a paper using simple dip coating method with enhanced stability. Moreover, the conductivity of PEDOT: PSS based paper can be significantly enhanced and tuned by treatment with a desired solvent. Further, doping with some nanomaterial may modulate the performance of paper in terms of electrochemical kinetics or signal stability and sensitivity. The reduced graphene oxide (RGO) has recently aroused much interest for development of electrochemical sensors. This is due to excellent electrochemical properties and large 2D surface area. Its abundant defects and chemical groups facilitate charge transfer and thus ensure increased electrochemical activity.(Pumera 2011) Hence incorporation of RGO in the PEDOT:PSS matrix may further improve electrochemical performance of a desired paper sensor.(Gao et al. 2014; Zhang et al. 2014)

Cancer is currently a serious concern and a medical threat to the contemporary world. An estimated 14.1 million new cases of cancer and 8.2 million deaths were reported in 2012 necessitating early diagnosis of this dreaded disease. (Cancer 2012) Carcinoembryonic antigen (CEA) is known to be a tumor marker associated with colon, lung, ovarian and breast cancer that

are responsible for more than half of all cancer deaths each year. (Kulpa et al. 2002; Myers et al. 1978; Pepe et al. 2001; Wanebo et al. 1978) In this context, determination of CEA in serum has been proposed for clinical diagnosis and monitoring of a cancer.

We report a facile method to obtain enhanced conductivity (~300 times) of PEDOT:PSS coated paper on treatment with ethylene glycol. Further, incorporation of RGO into the solution processed conducting paper results in improved electrochemical characteristics. This low cost, flexible and environment friendly conducting paper platform reveals high sensitivity towards a cancer biomarker (carcinoembryonic antigen, CEA) detection in the physiological range.

2. Materials and methods

2.1 Fabrication of PEDOT:PSS based conducting paper

The conducting paper (1cm×3cm) was prepared using a simple dip coating method. The PEDOT:PSS aqueous solution (1.3 wt%, PEDOT content 0.5 wt.%, PSS content 0.8 wt.%) purchased from Sigma Aldrich was ultrasonicated prior to use after which 3% ethylene glycol (EG) was added to the aqueous suspension of PEDOT: PSS. This solution was used to dip coat the Whatman filter paper #1 (procured from GE healthcare UK) rendering it conductive. It was then dried in a hot air oven at 100 °C and was termed as conducting paper.

2.2 Fabrication of PEDOT:PSS/RGO based electroactive paper

Preparation of the reduced graphene oxide (RGO) and PEDOT: PSS/RGO composite is given in supporting information. The Whatman paper (1cm×1cm) was dipped in PEDOT:PSS/RGO aqueous suspension (PEDOT:PSS content 1.3 wt%, RGO content 0.035wt%) containing 3% EG for 1 h and then dried at 100 °C in a hot air oven. Thereafter it was treated with EG by dipping in the EG solution for 20 min. The EG treated conducting paper finally dried at 100 °C for about 1 hr. A Schematic of the experiment has been demonstrated in Figure 1.

2.3 Characterization

The conductivity of the conducting paper was measured using the four points probe technique with a low current source (LCS-02), digital microvoltmeter (DMV-001) and PID controlled oven (PID-200), SES Instruments, India. The surface morphology was investigated by the high-resolution field emission scanning electron microscopy (Nova Nano Sem450, FEI). The transmission electron microscopy (TEM) was carried out with a JEM-2200 FS (JEOL, Japan). X-ray photoelectron spectroscopy (XPS) studies were performed using Axis-Nova, Kratos Analytical Ltd., Manchester, UK. The electrochemical studies were carried out by an Autolab Potentiostat/Galvanostat (Metrohm, Netherlands) using a conventional three-electrode cell with the electroactive paper as working electrode, platinum as auxiliary electrode and Ag/AgCl as the reference electrode in phosphate buffer saline (PBS, 50 mM, pH 7.4) containing 5 mM $[Fe(CN)6]^{3-/4-}$.

3. Results and Discussion

3.1 Electron Microscopy and elemental analysis

Transmission electron micrograph of the RGO exhibits curved sheet like structure with a fairly smooth surface (Figure 2A). The observed lighter and darker regions indicate the presence of RGO. The lighter region pertains to a few layered graphene whereas the darker region corresponds to the multilayerd graphene. The wrinkles and folds pertaining to the graphene sheet (sub-microns in size) are clearly visible. The selected area electron diffraction (SAED) pattern of RGO reveals hexagonal atomic structure and crystalline nature of the RGO sheets (Figure 2B). The inner six member ring represents the [1100] plane. The visible six diffraction spots corresponding to [0001] indicate hexagonal symmetry of the [0001] diffraction of the RGO.(Cui

et al. 2011) The RGO sheets appear to be uniformly covered with PEDOT: PSS (Figure 2C). The PSS molecules perhaps assist RGO dispersion via edge-to-face aromatic interactions between the RGO surface and the aromatic rings of the polymer which inhibits the hydrophobic graphene nanoplates from agglomeration, leading to a stable RGO dispersion in the polar solvent. (Hyun et al. 2013) The diffused ring like structure observed (Figure 2D) in the SAED pattern of PEDOT:PSS/RGO composite is because of the amorphous nature of PEDOT:PSS covering the RGO sheets. The SEM of PEDOT: PSS (Figure 2E) coated paper indicates uniform adsorption of PEDOT: PSS over cellulose fibers of the paper. Because of the high porosity and tiny interfiber air spaces in Whatman paper, the PEDOT:PSS adsorbs into the paper through capillary action and after drying it produces uniform and stable film of PEDOT:PSS on the paper. Figure 2F shows SEM of PEDOT: PSS/RGO coated paper. PEDOT: PSS/RGO is found to be uniformly adsorbed onto the cellulose fiber wherein some of RGO sheets are entangled in the fibrous network of Whatman paper. To further validate the formation of RGO, and its presence in PEDOT:PSS matrix, electron microscopic studies (SEM, elemental mapping and EDX) of RGO, PEDOT:PSS and PEDOT:PSS/RGO have been carried out (Supporting Information Figure S1).

3.2 Conductivity Studies

The PEDOT:PSS coated paper shows conductivity of 1.16×10^{-4} Scm^{-1} (see Supporting information for conductivity calculation). However, on addition of 3% ethylene glycol (EG) in PEDOT:PSS solution, the value of conductivity increases to 1.43×10^{-3} Scm^{-1}. This is due to decreased columbic interactions between PEDOT and PSS molecules that perhaps contribute to reorientation of the polymer chains resulting in improved charge carrier mobility.(Ouyang et al. 2005) Further, all studies have been done with PEDOT:PSS doped with 3% EG.(Wei et al. 2013)

The PEDOT:PSS doped with 3% EG coated Whatman paper has been termed as conducting paper.

The enhancement in the conductivity of PEDOT:PSS film (coated on glass substrate) has been recently reported when the film is dipped in methanol and H_2SO_4.(Alemu et al. 2012; Xia et al. 2012) This is due to ejection of the PSS ions from the PEDOT:PSS film dipped in the solvent, inducing the conformational rearrangement of PEDOT chains leading to higher conductivity. In the present case, effect of solvents such as methanol, H_2SO_4 and ethylene glycol (EG) on electrical conductivity of the conducting paper has been investigated (Supporting Information Table S1). We have observed that on flexible substrate (Whatman paper 1), EG treatment shows the highest value of conductivity (3.57×10^{-2} Scm^{-1}) in comparison to methanol (6.8×10^{-3} Scm^{-1}), and H_2SO_4 (8.1×10^{-3} Scm^{-1}). This is in accordance with a similar report wherein the effect of flexibility of material and polyelectrolyte adhesion to substrate was studied.(Podsiadlo et al. 2007) The increased flexibility of the EG treated conducting paper due to ejection of PSS results in the strong non-covalent cooperative interactions between PEDOT and cellulose molecules leading to higher conductivities. We have incorporated RGO in the PEDOT:PSS matrix for electrochemical studies since RGO exhibits excellent electrochemical properties.(Pumera 2011) PEDOT:PSS/RGO based conducting paper dipped in EG (electroactive paper) shows almost similar conductivity value (3.12×10^{-2} Scm^{-1}). The as-prepared electroactive paper shows greater degree of flexibility and efficient conductivity as demonstrated in figure 3.

The effect of folding (-180° to 180°), repeated folding and unfolding on conductivity of the electroactive paper has been investigated. Figure 3D describes results of flexibility studies conducted on the electroactive electrode; wherein the positive and negative angle clearly reveal electrode folding in upward and downward direction, respectively. Relative conductivity [(ratio

of measured conductivity (σ_{meas}) to initial conductivity (σ_o)] of electroactive electrode is measured as a function of folding angle. Figure 3E displays variation of the relative conductivity of electroactive electrode indicating deviation of upto 4% under different folding angles. This reveals that electrodes are flexible and there is negligible change in the conductivity. The variation of relative conductivity of electrode with repeated cycle of folding and unfolding (manually) is shown in figure 3F. It may be noted that the conducting paper folded after 30 cycles (1 cycle = 360° rotation) shows decrease of about 20% in relative conductivity due to tearing of the cellulose threads. A video pertaining to the lighting of an LED lamp when current is passed through the multiple times folded electroactive paper is shown in movie S1 in the Supporting Information.

Figure 4A represents Schematic of the observed mechanism, showing enhanced conductivity of the EG treated conducting paper. The conducting paper comprises of PEDOT:PSS polymer chains wherein PEDOT molecules present in the core of the insulating PSS are highly conductive in nature. On being treated with ethylene glycol, the core-shell structure of the conducting paper becomes partially linear due to ejection of the PSS molecules. This exclusion of PSS from the surface is perhaps responsible for conformational changes in the polymer film that in turn results in increased conductivity. This has been further confirmed by Fourier transform infrared (FT-IR) spectroscopy and X-ray photoelectron spectroscopy (XPS) studies.

3.3 FT-IR and XPS Analysis

FT-IR spectra of PEDOT:PSS/Whatman paper (curve i), conducting paper (curve ii) and conducting paper treated with EG (curve iii) are shown in Figure 4B. FT-IR spectrum of PEDOT:PSS coated on Whatman paper (spectra i) exhibits characteristic absorption bands at

near 670 cm^{-1} and 1060 cm^{-1}, corresponding to C-S and C-O stretching vibration of the thiophene ring in PEDOT. (Ely et al. 2014) The bands at 1010 cm^{-1}, 1045 cm^{-1} and 1160 cm^{-1} represent $–SO_3^-$ symmetric and asymmetric stretching vibrations, respectively due to PSS.(Alemu et al. 2012) The bands seen at 1392 cm^{-1} and 1537 cm^{-1} are due to C-C and C=C, respectively. In the FT-IR spectrum of conducting paper (curve ii), the intense absorption band at 1060 cm^{-1} is due to addition of EG that causes conformational changes in the polymer structure. The absorption band at 1104 cm^{-1} and 1160 cm^{-1} represent $–SO_3^-$ asymmetric stretching vibration whereas disappearance of $–SO_3^-$ symmetric stretching suggests molecular rearrangement in the PEDOT:PSS leading to increased electrical conductivity. These results are in agreement with those observed for the conductivity measurements wherein increase in conductivity from ~1.16×10^{-4} Scm^{-1} to ~1.43×10^{-3} Scm^{-1} occurs when EG is added into PEDOT:PSS. In the FT-IR of the EG treated conducting paper (curve iii), the characteristic bands seen at 1104 cm^{-1} and 1160 cm^{-1} pertaining to the $-SO^{3-}$ stretch of PSS are absent. This indicates removal of PSS from the conducting paper after EG treatment. This removal of PSS after EG treatment is perhaps responsible for the higher conductivity of the conducting paper due to increased exposure of PEDOT. FT-IR spectra of electroactive paper (Figure S2(i) in Supporting Information) indicates an additional broad absorption band at 1106 cm^{-1} that is attributed to C-OH stretching of graphene oxide. Further, the other observed IR bands are the same as seen in curve iii.

Figure 4C shows XPS of i) conducting paper ii) EG treated conducting paper. The S(2p) binding energy peak seen at 168 eV corresponds to sulfur due to presence of PSS, and the doublet peak seen at 163.8 eV and 164.5 eV correspond to the presence of sulfur in PEDOT.(Crispin et al. 2006) The S2p XPS intensity ratio of PEDOT/PSS increases from 0.721 to 0.760 after the conducting paper is treated with EG. This change indicates the removal of

some PSS chains from the film. That may perhaps cause conformational change in PEDOT:PSS due to the transition from coiled to linear form leading to increased exposure of PEDOT chains (Figure 3A).(Alemu et al. 2012) The change in C/S molar ratio evaluated from the scan spectra decreases from 9.63 to 8.17 after the conducting paper is treated with EG, is consistent with the removal of some PSS from the film. XPS of electroactive paper is shown in Figure S2(ii) (See Supporting Information).The S2p XPS intensity ratio of PEDOT/PSS present in electroactive paper increases to 0.82. However, the conductivity of electroactive paper is almost equivalent to that of the conducting paper after EG treatment. This may perhaps be attributed to the presence of discontinuous and non-uniform RGO sheet resulting in increased distance between PEDOT chains within the fiber network. Further, the C/S molar ratio increases to 10.1 due to presence of carbon content of RGO.

3.4 Electrochemical studies

To investigate the charge transfer phenomenon at the conducting paper/solution interface, the electrochemical impedance spectroscopy (EIS) studies have been conducted at biasing potential of 0.01V in the frequency range, 100 KHz to 1Hz. The Randles circuit is an equivalent electrical circuit that is commonly used to measure the electrochemical impedance comprising of an active electrolyte resistance R_S in series with R_{ct} (charge transfer resistance) in parallel combination of the double-layer capacitance C_{dl} or constant phase element (CPE) of a Faradaic reaction. The diameter of the semicircle in the Nyquist plot gives magnitude of the charge transfer resistance (R_{ct}) at the electrode surface. (Daniels and Pourmand 2007) Figure 5A shows EIS of the (i) conducting paper, (ii) conducting paper treated with EG, (iii) electroactive paper. Figure 5A, has been obtained using software (Nova) provided with the Autolab

Potentiostat/Galvanostat. The curve fitting has been done assuming Randles circuit [$R_s(R_{ct}\ C_{dl})$] of the electrochemical cell. The various parameters related to the circuit element have been summarized in Table S2 alongwith % error [see supplementary information sheet]. The R_{ct} obtained for conducting paper is 48 kΩ which is maximum (curve i). However, the significant decrease in R_{CT} value upto 7 kΩ (curve ii) is observed in EG treated conducting paper. This is assigned to the conformational changes of the PEDOT:PSS chains from coiled to linear form leading to the higher conductivity due to enhanced electron transfer between solution/electrode interface. It is observed that the R_{ct} value further decreases to 2.8 kΩ (curve iii) in case of the electroactive paper. This may be attributed to excellent electrochemical properties and larger 2D surface area of RGO incorporated in the PEDOT:PSS matrix that increases the permeability of $[Fe(CN)_6]^{3-/4-}$ to the surface of paper electrode. The heterogeneous electron transfer rate constant (K_{ct}) of EG treated conducting paper and electroactive paper has been calculated using Equation 1. (Bardea et al. 2000)

$$K_{ct} = \frac{RT}{n^2F^2AR_{ct}[S]} \quad \text{.....(1)}$$

where R is the gas constant, T is absolute temperature, F is the Faraday constant, A is the electrode area (cm^2), [S] is the concentration of redox probe (mol/cm^3) and n is the number of transferred electron per molecule of the redox probe. The heterogeneous electron transfer rate constant (Kct) value of the electroactive paper has been estimated as 1.9×10^{-5} cm s^{-1} which is 2.5 times better as compared to conducting paper treated with EG (7.6×10^{-6} cm s^{-1}). This indicates that the RGO present in electroactive paper electrode exhibits faster electron transfer kinetics as compared to the EG treated conducting paper. Thus the incorporation of RGO improves the

electrochemical activity of the electroactive paper as compared to that of EG treated conducting paper.

Figure 5B shows results of the chronoamperometric studies (current *verses* time) conducted on conducting paper and EG treated conducting paper at 2V every 0.1s .The higher value of the current observed for EG treated conducting paper electrode than that of conducting paper indicates increased electron transfer between solution and electrode due to conformational rearrangement in PEDOT polymeric chains. Further increase in the value of the electrochemical current in case of the electroactive paper electrode is attributed to the enhancement in permeability of the redox couple $[Fe(CN)_6]^{3-/4-}$ resulting due to RGO doping. It may be noted that electroactive paper electrode exhibits improved electrochemical performance and signal stability than that of the EG treated conducting paper. Keeping this in view, electroactive paper has been used to detect cancer biomarker, CEA. The monoclonal carcinoembryonic antibodies (anti-CEA) (procured from Sigma Aldrich) are physically absorbed onto the PEDOT:PSS/RGO based electroactive paper [Figure 1]. The anti-CEA immobilized paper bioelectrode is washed with phosphate buffer (PBS. 50 mM, 0.9% NaCl; pH 7.4) to remove any unbound antibodies. Different concentrations of the carcinoembryonic antigen (CEA) (1-10 $ngmL^{-1}$) are prepared via further dilution of stock solution (25μgmL^{-1}). The response studies of anti-CEA/electroactive paper obtained as a function of CEA concentration (1-10 $ngmL^{-1}$), have been carried out in phosphate buffer saline (PBS, 50 mM, pH 7.4) containing 5 mM $[Fe(CN)6]^{3-/4-}$. 10µL of diluted antigen solution is added into electrochemical cell for each antigen concentration. After adding each CEA concentration the current-time curve is recorded after every 300 s to ensure completion of the immunoreaction. The variation of the response current recorded as a function of CEA (1-10 $ngmL^{-1}$) is shown in Figure 5C. The decrease in amperometric current occurs upto

a maximum of 10 ngmL^{-1}. This can be attributed to the formation of antigen–antibody complex causing significant rearrangement over the electrode surface that diminishes charge transfer via $[Fe(CN)_6]^{3-/4-}$ leading to reduction in amperometric current. (Shim et al. 2008; Wang et al. 2009) Figure 5D indicates the calibration plot obtained between response current and CEA concentration (curve i). Interestingly, we obtained similar results between electrochemical current and CEA concentration via single shot incubation (different electrode was taken for each concentration) is shown in figure S3. Furthermore, a control experiment has been performed to check cross reactivity of the electroactive paper with CEA antigen in the absence of antibodies (curve ii). However, no significant change in current response is observed for the electroactive paper in the absence of antibodies as a function of CEA concentration. A linear relationship is observed in the range 2-8 ngmL^{-1} with a sensitivity of 25.8 μAng^{-1}mLcm^{-2} and follows the Equation (2).

$$I(A) = -25.8\ \mu A\ mL\ ng^{-1} \times [CEA\ concentration] + 613.5\ \mu A;\ R^2 = 0.998 \quad \ldots. (2)$$

We have compared the sensing performance of the electroactive paper with the conducting paper treated with EG. For this, the electrochemical response studies have been carried out on the anti-CEA immobilized conducting paper treated with EG, in presence of different concentration of antigen (1-10 ng/ml) (See supporting information figure S4). It is found that the electroactive paper is almost 6 times more sensitive than the conducting paper treated with EG for CEA detection.

3.5 Stability, Selectivity and Reproducibility studies

Figure 6A shows variation of response current of the immunoelectrode (anti-CEA immobilized electroactive paper) taken at a regular interval of 2 days. It has been found that current value decreases to ~7**%** after 21 days. This indicates that the paper sensor exhibits good

stability upto 21 days. The selectivity study of this paper sensor has been investigated in the presence of cardiac troponin I (cTnI), cytokeratin-19 fragment (CYFRA-21-1), and endotheline-1 protein (ET-1) ($2ngmL^{-1}$). Figure 6B shows decrease in current response on addition of CEA ($2ngmL^{-1}$) after which we do not observe any significant current change on addition of other antigen indicating high selective of the biosensor. The reproducibility of the five different immunoelectrodes fabricated under similar conditions has been investigated in presence of $2ngmL^{-1}$ CEA concentration (Figure 6C). It is found that this paper electrode shows good reproducibility for five different electrodes with constant surface area as is evident by low value of relative standard deviation (RSD) of 7.6% (mean value = 609μA). Further each measurement (figure 6C) has been repeated 4 times for each electrode and error bars are included accordingly. The low RSD obtained for each electrode (less than 5 %) indicates appreciable repeatability of the biosensor.

3.6 Real sample analysis

The results obtained for serum sample of cancer patients using this electroactive paper sensor have been validated using ELISA. The blood samples collected from patient and processed at the Rajiv Gandhi Cancer Institute & Research Centre (RGCI & RC) in Rohini, Delhi, India. Concentration of CEA in the serums of cancer patients were measured at RGCI&RC using the VITROS CEA reagent Pack and the VITROS CEA Calibrators on the VITROS ECi/ECiQ Immunodiagnostic Systems, VITROS 3600 Immunodiagnostic System and VITROS 5600 Integrated System using Intellicheck® Technology. It can be seen that a reasonable correlation occurs between the CEA concentration value obtained by immunoassay and the electroactive paper based electrochemical method (Figure 6D). As shown in Figure 6D, the electroactive paper affords good recoveries and acceptable relative standard deviation.

The sensing characteristics of the electroactive paper based electronic paper sensor have been summarized in Table S3 along with those reported in literature. It may be noted that this low cost flexible electroactive paper sensor can be easily decomposed by simple incineration (See Movie S2). Keeping in view the production of the medical diagnostics kits, this is an added advantage of this new environment friendly disposable electroactive paper sensor.

Conclusions

We have demonstrated a flexible and highly conducting paper sensor, based on composite of poly(3,4-ethylenedioxythiophene):poly(styrenesulfonate) (PEDOT:PSS) and reduced graphene oxide (RGO). It is found that conductivity of the PEDOT:PSS conducting paper increases by ~300 times when it is treated with ethylene glycol. The incorporation of RGO in PEDOT:PSS conducting paper film indicates excellent electrochemical activity and faster charge transfer kinetics. In order to further improve the performance of conducting paper, suitable selection of solvent and dopant are under extensive investigation. This low cost, flexible and environment friendly conducting paper has been used for cancer biomarker detection. The fabricated PEDOT:PSS/RGO based electroactive paper shows sensitivity of 25.8 $\mu A ng^{-1} mL cm^{-2}$ in the detection range of 2-8 $ngmL^{-1}$. The results obtained for serum samples of cancer patients using this paper based sensor have been validated using ELISA. This simple, low cost, flexible and disposable electroactive paper based platform has immense potential for point of care biosensors, flexible electronics and energy storage devices etc.

Acknowledgements

We thank Prof. Pradeep Kumar, Vice Chancellor Delhi Technological University (DTU), Delhi, India for providing the facilities. Saurabh Kumar and Suveen Kumar are thankful to DTU

for the award of financial assistance. We would like to thank to support by the National Research Foundation of Korea (NRF) Grant funded by the Korean Government (MSIP) (2014R1A4A1008140).

References

Alemu, D., Wei, H.-Y., Ho, K.-C., Chu, C.-W., 2012. Highly conductive PEDOT: PSS electrode by simple film treatment with methanol for ITO-free polymer solar cells. Energy & environmental science 5(11), 9662-9671.

Bardea, A., Katz, E., Willner, I., 2000. Probing antigen–antibody interactions on electrode supports by the biocatalyzed precipitation of an insoluble product. Electroanalysis 12(14), 1097-1106.

Cancer, I.A.f.R.o., 2012. World Cancer Factsheet. World Health Organization, www. cancerresearchuk. org.

Crispin, X., Jakobsson, F., Crispin, A., Grim, P., Andersson, P., Volodin, A., Van Haesendonck, C., Van der Auweraer, M., Salaneck, W.R., Berggren, M., 2006. The origin of the high conductivity of poly (3, 4-ethylenedioxythiophene)-poly (styrenesulfonate)(PEDOT-PSS) plastic electrodes. Chemistry of Materials 18(18), 4354-4360.

Cui, P., Lee, J., Hwang, E., Lee, H., 2011. One-pot reduction of graphene oxide at subzero temperatures. Chemical Communications 47(45), 12370-12372.

Daniels, J.S., Pourmand, N., 2007. Label-Free Impedance Biosensors: Opportunities and Challenges. Electroanalysis 19(12), 1239-1257.

Dhand, C., Das, M., Datta, M., Malhotra, B., 2011. Recent advances in polyaniline based biosensors. Biosensors and Bioelectronics 26(6), 2811-2821.

Ely, F., Matsumoto, A., Zoetebier, B., Peressinotto, V.S., Hirata, M.K., de Sousa, D.A., Maciel, R., 2014. Handheld and automated ultrasonic spray deposition of conductive PEDOT: PSS films and their application in AC EL devices. Organic Electronics 15(5), 1062-1070.

Gao, Y., Li, J., Yang, X., Xiang, Q., Wang, K., 2014. Electrochemiluminescence Biosensor Based on PEDOT-PSS-Graphene Functionalized ITO Electrode. Electroanalysis 26(2), 382-388.

Gervais, L., De Rooij, N., Delamarche, E., 2011. Microfluidic Chips for Point-of-Care Immunodiagnostics. Advanced Materials 23(24), H151-H176.

Hyun, W.J., Park, O.O., Chin, B.D., 2013. Foldable graphene electronic circuits based on paper substrates. Advanced Materials 25(34), 4729-4734.

Jagadeesan, K.K., Kumar, S., Sumana, G., 2012. Application of conducting paper for selective detection of troponin. Electrochemistry Communications 20, 71-74.

Kulpa, J., Wójcik, E., Reinfuss, M., Kołodziejski, L., 2002. Carcinoembryonic antigen, squamous cell carcinoma antigen, CYFRA 21-1, and neuron-specific enolase in squamous cell lung cancer patients. Clinical chemistry 48(11), 1931-1937.

Kumar, S., Jagadeesan, K.K., Joshi, A.G., Sumana, G., 2013a. Immuno-CoPS (conducting paper strips) for futuristic cost-effective cancer diagnostics. RSC Advances 3(29), 11846-11853.

Kumar, S., Kumar, S., Ali, M., Anand, P., Agrawal, V.V., John, R., Maji, S., Malhotra, B.D., 2013b. Microfluidic-integrated biosensors: Prospects for point-of-care diagnostics. Biotechnology journal 8(11), 1267-1279.

Li, L., Wang, Y., Pan, L., Shi, Y., Cheng, W., Shi, Y., Yu, G., 2015. A nanostructured conductive hydrogels-based biosensor platform for human metabolite detection. Nano letters.

Luppa, P.B., Müller, C., Schlichtiger, A., Schlebusch, H., 2011. Point-of-care testing (POCT): Current techniques and future perspectives. TrAC Trends in Analytical Chemistry 30(6), 887-898.

Myers, R.E., Sutherland, D.J., Meakin, J.W., Kellen, J.A., Malkin, D.G., Malkin, A., 1978. Carcinoembryonic antigen in breast cancer. Cancer 42(S3), 1520-1526.

Ouyang, J., Chu, C.W., Chen, F.C., Xu, Q., Yang, Y., 2005. High-Conductivity Poly (3, 4-ethylenedioxythiophene): Poly (styrene sulfonate) Film and Its Application in Polymer Optoelectronic Devices. Advanced Functional Materials 15(2), 203-208.

Pepe, M.S., Etzioni, R., Feng, Z., Potter, J.D., Thompson, M.L., Thornquist, M., Winget, M., Yasui, Y., 2001. Phases of biomarker development for early detection of cancer. Journal of the National Cancer Institute 93(14), 1054-1061.

Podsiadlo, P., Tang, Z., Shim, B.S., Kotov, N.A., 2007. Counterintuitive effect of molecular strength and role of molecular rigidity on mechanical properties of layer-by-layer assembled nanocomposites. Nano letters 7(5), 1224-1231.

Pumera, M., 2011. Graphene in biosensing. Materials today 14(7), 308-315.

Shim, B.S., Chen, W., Doty, C., Xu, C., Kotov, N.A., 2008. Smart electronic yarns and wearable fabrics for human biomonitoring made by carbon nanotube coating with polyelectrolytes. Nano letters 8(12), 4151-4157.

Tobjörk, D., Österbacka, R., 2011. Paper electronics. Advanced Materials 23(17), 1935-1961.

Wanebo, H.J., Rao, B., Pinsky, C.M., Hoffman, R.G., Stearns, M., Schwartz, M.K., Oettgen, H.F., 1978. Preoperative carcinoembryonic antigen level as a prognostic indicator in colorectal cancer. New England Journal of Medicine 299(9), 448-451.

Wang, J., 2006. Electrochemical biosensors: towards point-of-care cancer diagnostics. Biosensors and Bioelectronics 21(10), 1887-1892.

Wang, L., Chen, W., Xu, D., Shim, B.S., Zhu, Y., Sun, F., Liu, L., Peng, C., Jin, Z., Xu, C., 2009. Simple, Rapid, Sensitive, and Versatile SWNT− Paper Sensor for Environmental Toxin Detection Competitive with ELISA. Nano letters 9(12), 4147-4152.

Wei, Q., Mukaida, M., Naitoh, Y., Ishida, T., 2013. Morphological Change and Mobility Enhancement in PEDOT: PSS by Adding Co-solvents. Advanced Materials 25(20), 2831-2836.

Xia, Y., Sun, K., Ouyang, J., 2012. Solution-Processed Metallic Conducting Polymer Films as Transparent Electrode of Optoelectronic Devices. Advanced Materials 24(18), 2436-2440.

Zhai, D., Liu, B., Shi, Y., Pan, L., Wang, Y., Li, W., Zhang, R., Yu, G., 2013. Highly sensitive glucose sensor based on Pt nanoparticle/polyaniline hydrogel heterostructures. ACS nano 7(4), 3540-3546.

Zhang, M., Yuan, W., Yao, B., Li, C., Shi, G., 2014. Solution-Processed PEDOT: PSS/Graphene Composites as the Electrocatalyst for Oxygen Reduction Reaction. ACS applied materials & interfaces 6(5), 3587-3593.

Figure 1. Schematic of proposed electroactive paper sensor.

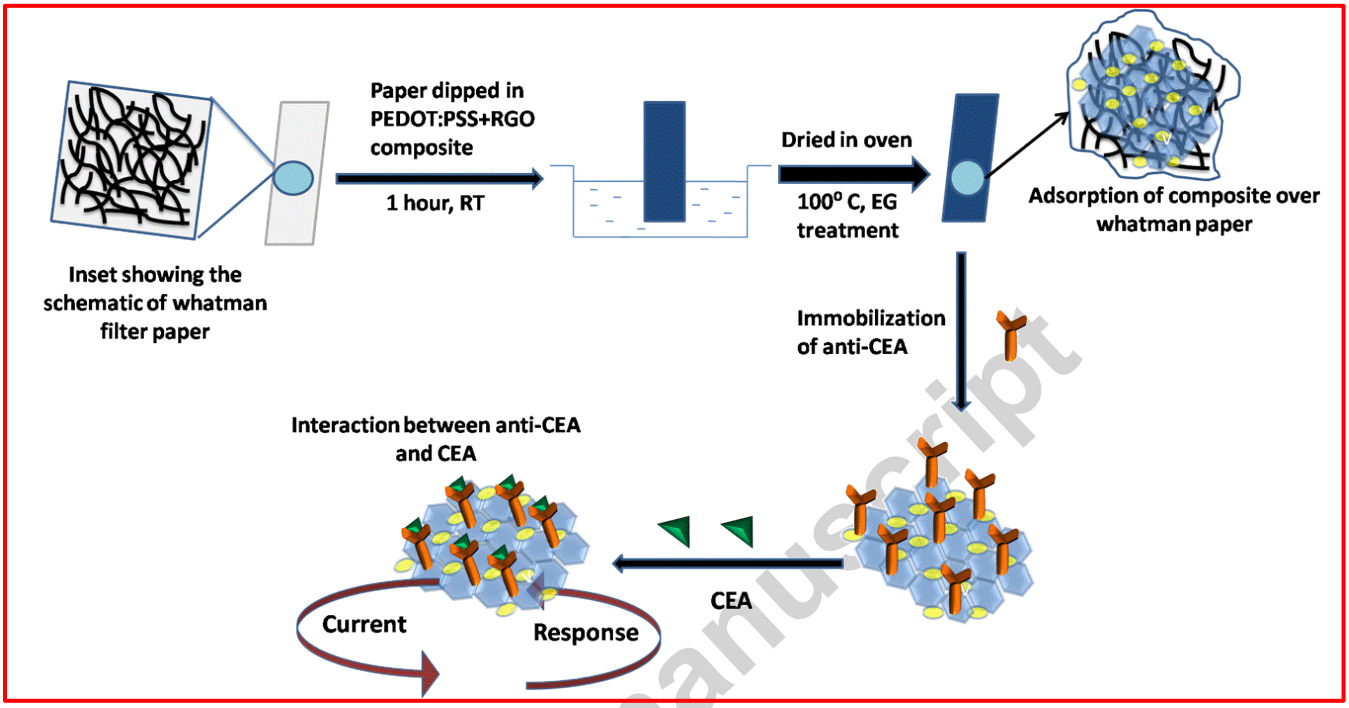

Figure 2. (A) TEM image of synthesized reduced graphene oxide (RGO) where darker region correspond to multilayer and lighter region corresponds to a few layer graphene (B) SAED of RGO, which confirms the hexagonal atomic structure and crystalline nature of the sheets. (C) TEM image of PEDOT:PSS/RGO. (D) SAED pattern of PEDOT:PSS/RGO composite (E) SEM of PEDOT:PSS adsorbed onto Whatman paper (F) SEM of PEDOT:PSS/RGO Whatman coated paper.

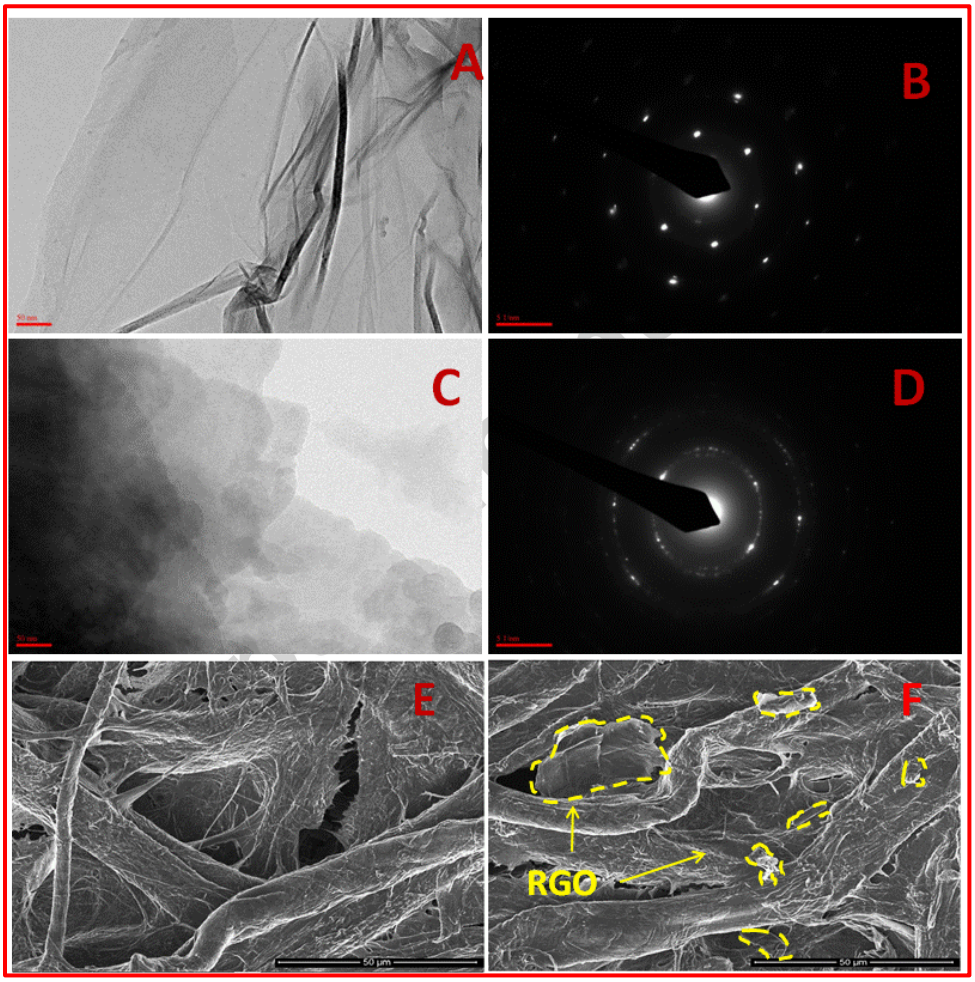

Figure 3. Optical image of electroactive paper (A) foldable nature of electroactive paper (B, C) demonstration of LED emission when current flow through electoactive paper. Flexibility studies of PEDOT:PSS/RGO based electroactive electrode (D) Schematic diagram of electrode folding at different deformation angle. (E) The ratio of measured conductivity (σ_{meas}) to initial conductivity (σ_o) of electroactive paper with respect to folding angle. (F) The ratio of measured conductivity (σ_{meas}) to initial conductivity (σ_o) of electroactive paper verses folding cycle (1 cycle = 360°).

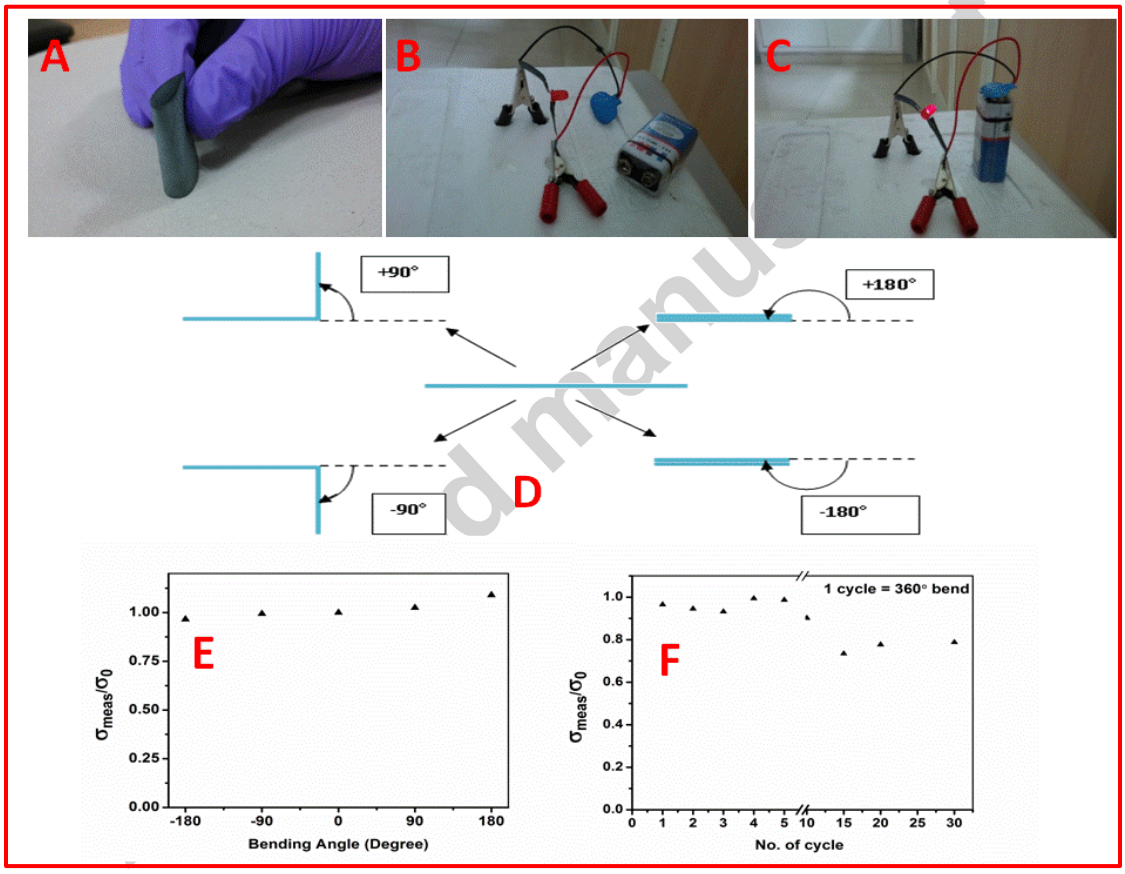

Figure 4. (A) The schematic illustration of the mechanism of conductivity enhancement on conducting paper surface by EG treatment. (B) The FT-IR spectra of (i) PEDOT: PSS/Whatman paper (ii) conducting paper (iii) conducting paper treated with EG (C) X-ray photoelectron spectra (XPS) of (i) conducting paper (ii) conducting paper treated with ethylene glycol.

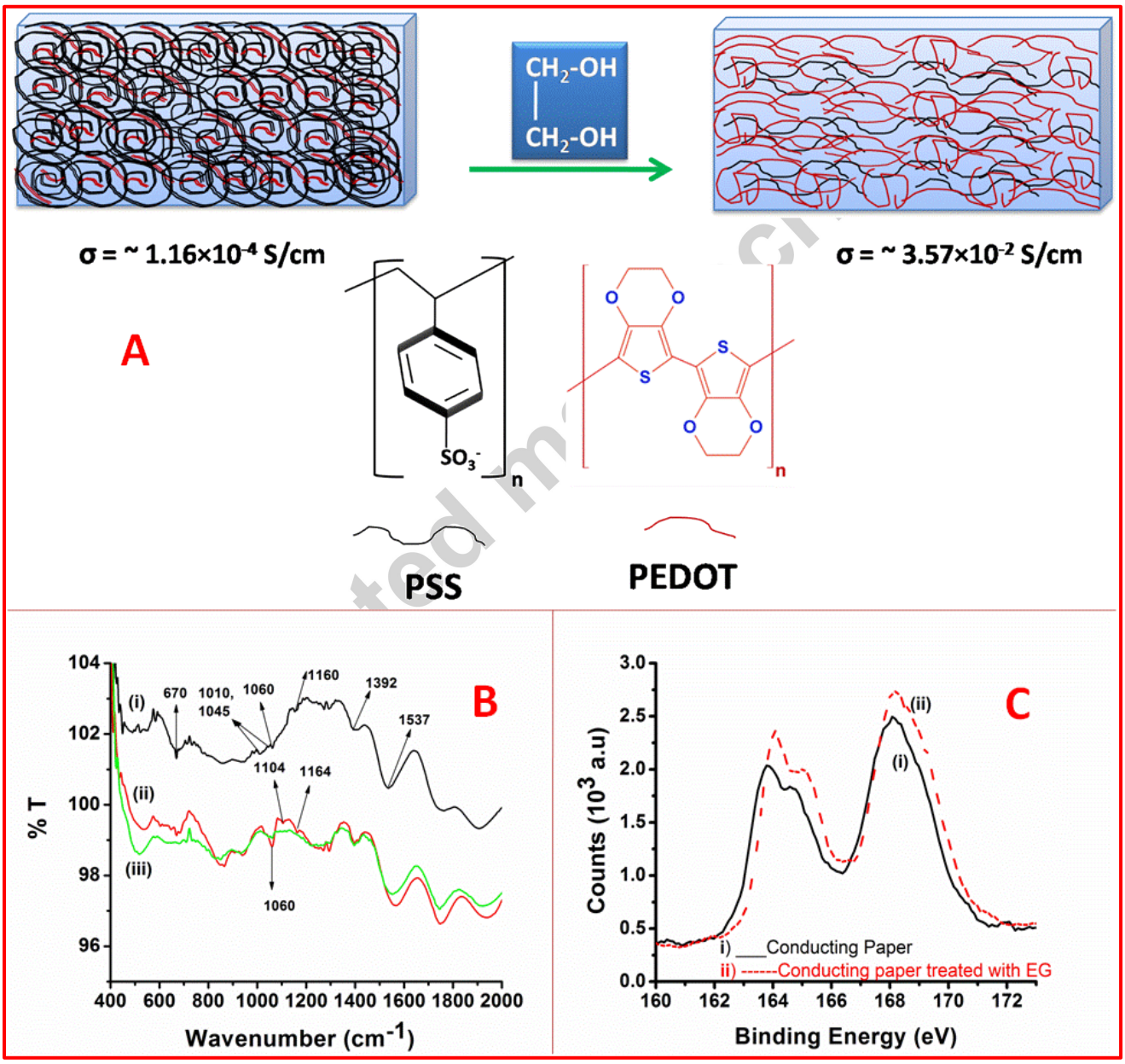

Figure 5. Electrochemical studies conducted on paper electrode (A) Electrochemical impedance spectra (B) Chronoamperometry plot obtained for (i) conducting paper (ii) conducting paper treated with EG (iii) electroactive paper (C) Electrochemical response studies of anti-CEA immobilized electroactive paper at different concentration of CEA (D) Calibration plot between the magnitudes of current recorded and CEA concentration (curve i); control experiment in absence of antibody (curve ii). Conducting paper: EG doped PEDOT: PSS solution coated onto whatman paper; Electroactive paper: EG and RGO doped PEDOT:PSS solution coated onto Whatman paper further treated with EG.

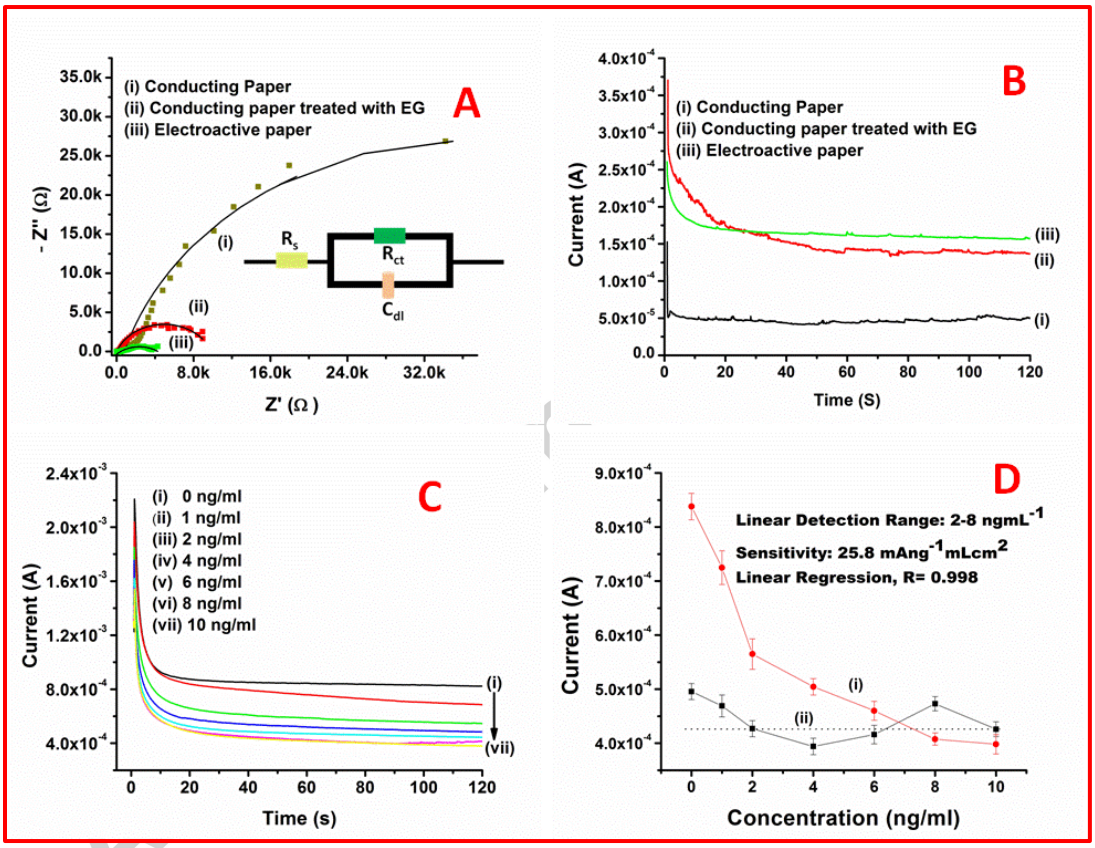

Figure 6. (A) Electrochemical current response of anti-CEA immobilized electroactive paper electrode (immunoelectrode) measured as a function of time (day) (B) Electrochemical current response of immunoelectrode in the presence of other analytes (C) Electrochemical current response of different immunoelectrode fabricated via the same set of procedure in presence of CEA (2 ng/ml) and (D) CEA concentration values obtained by immunoassay and the electroactive paper method.

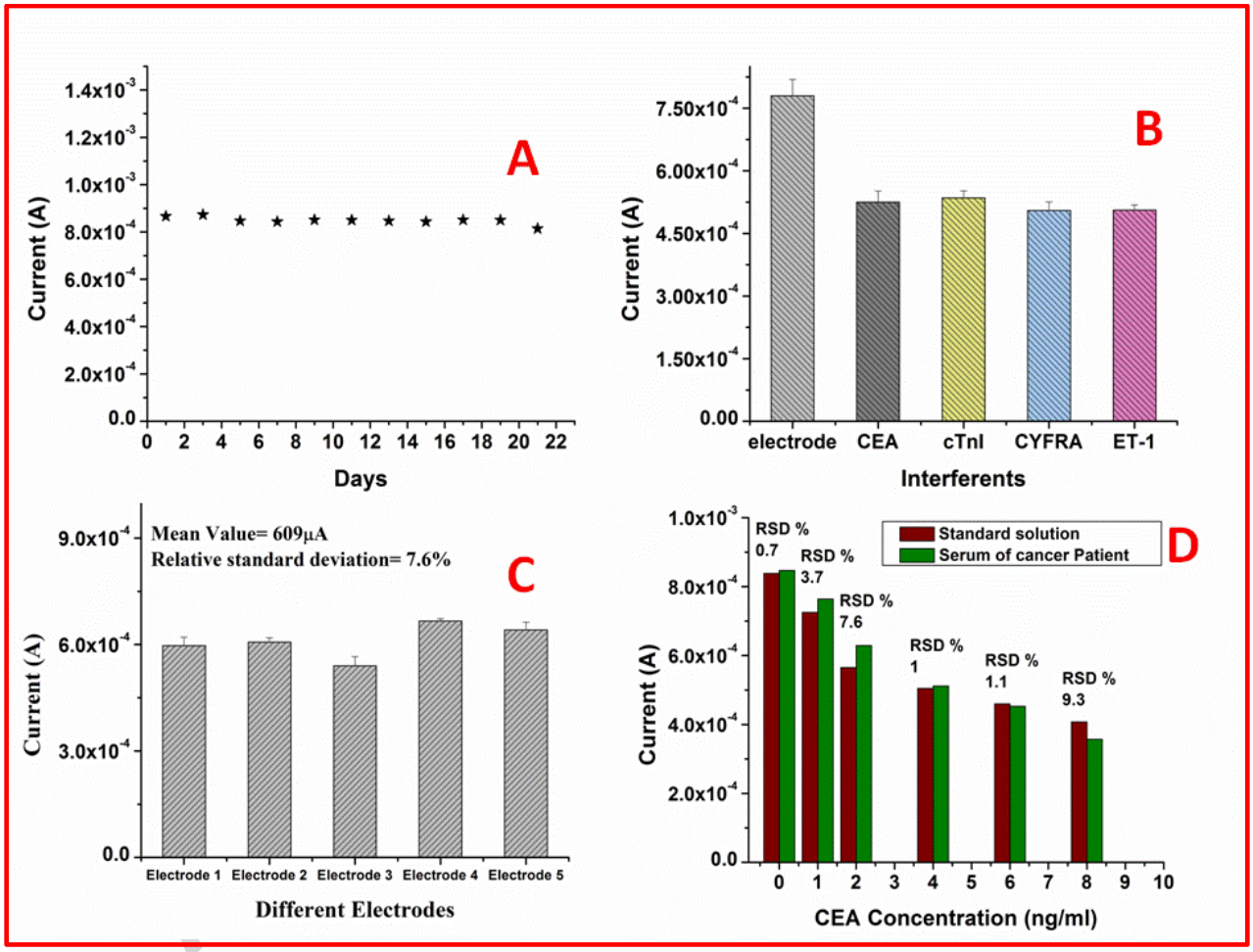

Highlights

1. Solution processed reduced graphene oxide modified conducting paper sensor has been reported for cancer detection.

2. It is exceptionally low cost, flexible and disposable

3. It exhibits high sensitivity of 25.8 μA $ng^{-1}mL\ cm^{-2}$ in the detection range of 1-10 $ngmL^{-1}$ for cancer biomarker (carcinoembryonic antigen, CEA) detection.

4. Owing to the efficient conductivity of the paper electrode, it may be a promising alternative over the expensive conventional electrodes (ITO, gold and glassy carbon) for its application in POC devices.

Supporting videos captions

Movie S1: A video indicating the lighting of an LED lamp when current is passed through the multiple times folded electroactive paper.

Movie S2: A video demonstrating that the electroactive paper sensor can be easily decomposed by simple incineration.